Flexibility versus rigidity: what determines the stability of zeolite frameworks? A case study

Supplementary Information

Elke Verheyen[a], Lennart Joos[b], Charlotte Martineau[c], Colby J. Dawson[d], Claudia Weidenthaler[e], Wolfgang Schmidt[e], Ruting Yuan[a], Eric Breynaert[a], Veronique Van Speybroeck[b], Michel Waroquier[b], Francis Taulelle[a,c], Michael M.J. Treacy[d], Johan A. Martens[a] and Christine E.A. Kirschhock[a]

[a] Centre for Surface Chemistry and Catalysis, KU Leuven, Kasteelpark Arenberg 23, Leuven, Belgium.

[b] Center for Molecular Modeling, Ghent University, 9052 Zwijnaarde, Belgium

[c] Tectospin, Institut Lavoisier de Versailles, UMR CNRS 8180 Université de Versailles St Quentin en Yvelines, 45 Avenue des Etats Unis, Versailles Cedex, France

[d] Department of Physics, Arizona State University, P.O. Box 871504, Tempe, USA.

[e] Max-Planck-Institut für Kohlenforschung, Kaiser-Wilhem-Platz 1, Mülheim an der Ruhr, Germany

Table of contents

Zeolite characterization

X-ray diffraction

Room temperature X-ray powder diffraction patterns were recorded in a rotating 0.5 mm glass capillary (Hilgenberg) on a STOE Stadi MP diffractometer with focusing Ge(111) monochromator (CuKα_1 radiation, λ = 1.54056 Å) in Debye-Scherrer geometry with a linear position sensitive detector (PSD) (6° 2theta window) from 6 to 35° 2theta, with a step width of 0.5 degree, internal PSD resolution of 0.01 degree, and an accumulation time of 400 s per step.

NMR

The solid-state nuclear magnetic resonance (NMR) spectra were recorded on an Avance 500 Bruker spectrometer (Larmor frequencies of 99.3 MHz) using a 4 mm probe at magic-angle spinning (MAS) frequency of 10 kHz. Single-pulse ^{29}Si NMR spectra were acquired with a 5 μs 90° pulse length. The recycle delay was 120 s, to ensure full return of the magnetization to equilibrium, and about 512 transients were recorded for each sample. The ^{29}Si chemical shifts were referenced to TMS. The spectra were deconvoluted with the Dmfit software[1].

Nitrogen adsorption

The porosity of the samples was determined using nitrogen adsorption at 77 K (Autosorb-1, Quantachrome). Prior to nitrogen adsorption, -COK-14(H1) and -COK-14(H2) were evacuated at 393 K for 12 h. The COK-14(C1) was pretreated at 573 K for 12 h. The micropore volume and micropore size distribution were analysed using the t-plot method[2] and the SF method[3], respectively.

High temperature X-ray diffraction

In situ XRD experiments were conducted with a PANalytical X'Pert Pro diffractometer equipped with an Anton Paar XRK900 high temperature reaction chamber. The system works in Bragg-Brentano geometry (Macor® sample holder, 6-10 mm diameter) with a Ni-filtered Cu K$\alpha_{1,2}$ radiation source (40 kV, 40 mA). A set of 0.04 rad primary and secondary soller slits, a 0.5° divergence slit and a 1° anti-scatter slit guarantees a good trade-off between intensity and resolution. Data were collected in the range between 5-32° 2theta with a step width of 0.017° 2theta and an acquisition time of 40 s per point. The measurements were performed under pure N_2 flow. Samples were heated from room temperature to 373 K with a heating rate of 2 K min^{-1}. For further heating a rate of 5 K min^{-1} was applied.

Thermogravimetric analysis

Thermal gravimetric analysis was performed on a TGA Q500 (TA instruments, Belgium) under nitrogen flow at a heating rate of 1 K min^{-1} from room temperature to 950 K.

Computational details

To obtain insight into the flexibility, stability and transformation of the interrupted -COK-14 and fully connected analogue COK-14, a variety of complementary simulations have been performed.

As first modeling technique, periodic density functional theory (DFT) calculations are performed. These simulations were performed with VASP (Vienna Ab Initio Simulation Package)[4,5], using projector-augmented waves[6,7] and a plane wave basis set to describe the electron density. The exchange-correlation functional is expressed by the generalized-gradient approximation with the Perdew-Burke-Ernzerhof (PBE) parametrization[8]. As the unit cell is relatively large, a gamma point sampling of the reciprocal space was used. In first instance, static DFT calculations determine the electronic ground state of the interrupted and condensed framework. Thermal corrections to the free energy and entropic contributions are extracted from a full vibrational analysis of the frequency calculations. The latter type of simulations is computationally very expensive, as high convergence criteria have to be used and the structure needs to be optimized several times in order to remove all negative frequencies.[9] In a first step, both the ions and the unit cell (volume and shape) are allowed to relax, until forces are converged to 0.001 eV/Å. Then, the unit cell is kept fixed and the ions are relaxed until forces are below 0.0005 eV/Å. Thirdly, a frequency calculation is performed and in case there are undesired negative frequencies, the process is reiterated. Three frequencies associated with the overall translation of the framework were projected out using the in-house software Tamkin.[10] For the relaxations, the plane wave cut-off was set to 600 eV and electronic convergence to 10^{-6} eV at highest. We used the energy of the last optimalization. For the frequency calculations, the cut-off was lowered to 400 eV, to retain a reasonable computational cost, electronic convergence was set to 10^{-6} eV and the step size of the vibrational analysis was 0.01 Å. The analysis is performed using the harmonic oscillator approximation and the water molecules which are released during the closing of the framework are treated in the gas phase. In this methodology the water molecules are fully recovering their overall rotational and translational degrees of freedom by closing of the framework.

A second set of simulations explores the geometric flexibility of these frameworks. Therefore the structures were optimized using the General Utility lattice Program (GULP)[11] with a Keating-type potential that favours Si-O bond distances of 1.610 Å, Ge-O bond distances of 1.756Å, and O-T-O angles of 109.471°. A structure is considered 'relaxed' when all T-O bond lengths are within ±0.001Å of the preferred bond length and within ±0.001° of the preferred O-T-O bond angle, with no overlapping oxygen atoms (assuming an oxygen radius of 1.31 Å). In a number of cases, it is necessary to lower the space group symmetry in order for full relaxation to occur. The empirical potential of Sanders-Leslie-Catlow (SLC)[12] was then used in GULP[11] to find framework energy-optimized structures when represented as pure silicates. The program FINDSYM was used to detect higher symmetry when structures were relaxed in *P*1 symmetry.[13]
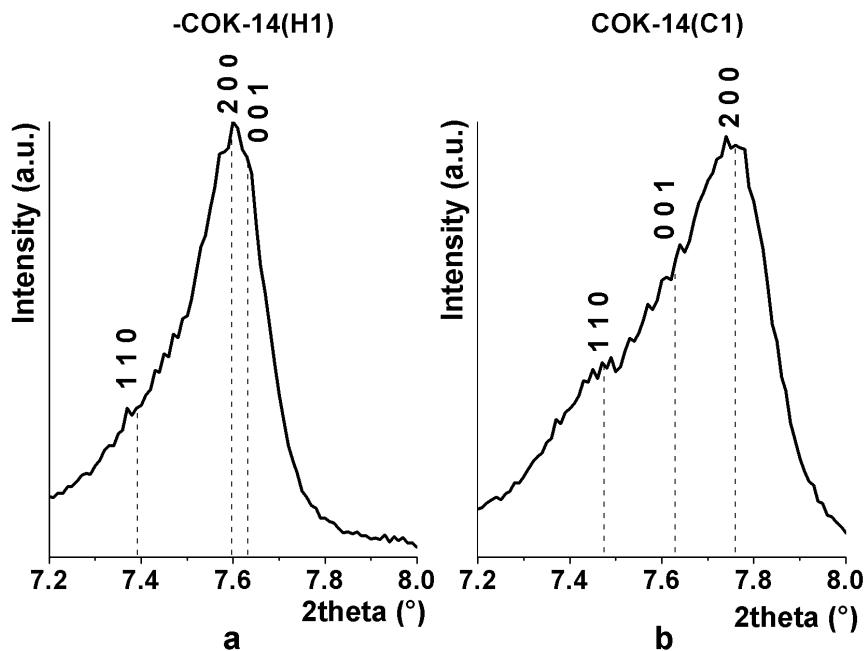
Figure S1

Figure S1 : X-ray diffraction pattern of (a) -COK-14(H1) and (b) COK-14(C1) in the 7.2 – 8° 2theta range. The position of the 1 1 0, 2 0 0 and the 0 0 1 reflection are indicated. A full list of all reflections of -COK-14(H1) and COK-14(C1), and corresponding ° 2theta positions can be found in Table S1. During transformation from -COK-14(H1) to COK-14(C1), the 1 1 0 reflection shifts from 7.39 to 7.49° 2theta, the 2 0 0 reflection from 7.60 to 7.77° 2theta and the position of the 0 0 1 reflection remains almost unchanged. The transformation from -COK-14 to COK-14 is most clearly visible in the shift of the 2 0 0 reflection.
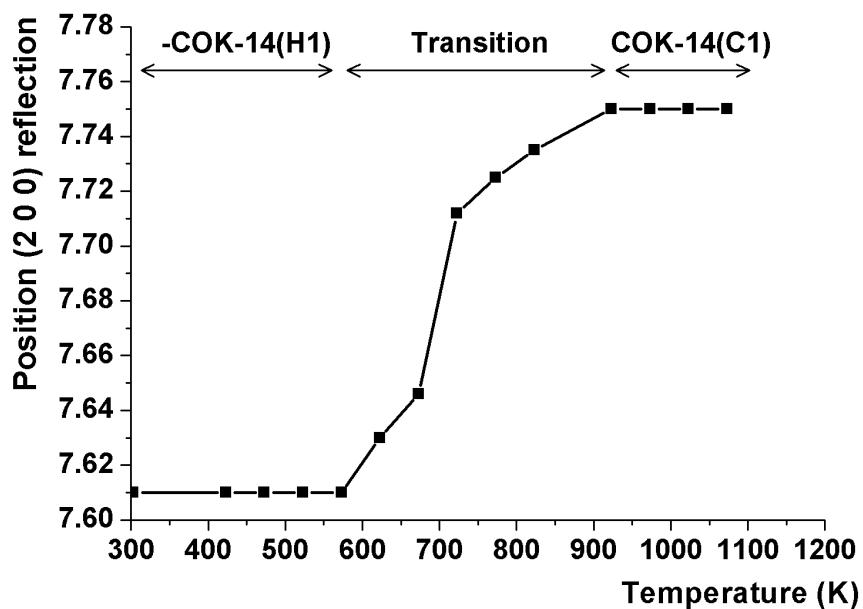
Figure S2 : Position of the 2 0 0 reflection in the transformation of -COK-14(H1) to COK-14(C1), obtained by high temperature XRD measurements recorded in 50 K intervals while heating from room temperature up to 1073 K under continuous nitrogen flow. The transition from -COK-14(H1) to COK-14(C1) clearly occurs in the temperature range 573 – 923 K.
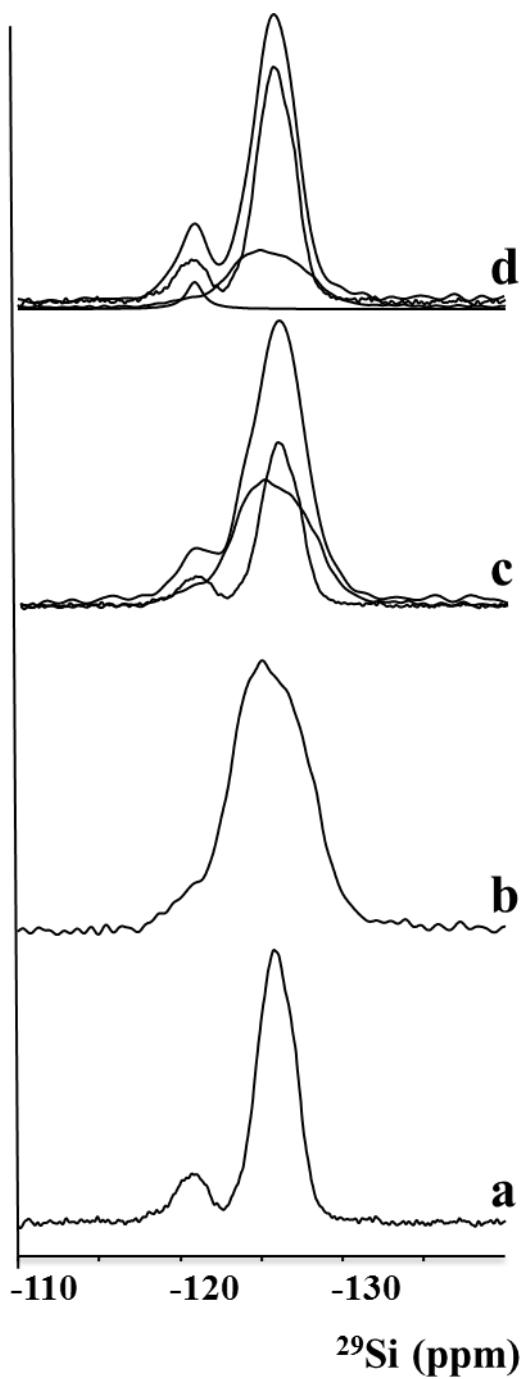
Figure S3 : ^{29}Si MAS NMR spectra of (a) -COK-14(H1), (b) COK-14(C1), (c) -COK-14(H2-43%) fitted as a linear combination of 43% -COK-14(H1) and 57% COK-14(C1) and (d) -COK-14(H2) fitted as a linear combination of 77% -COK-14(H1), 21% COK-14(C1) and 2% Q^3 silanols.

Figure S4
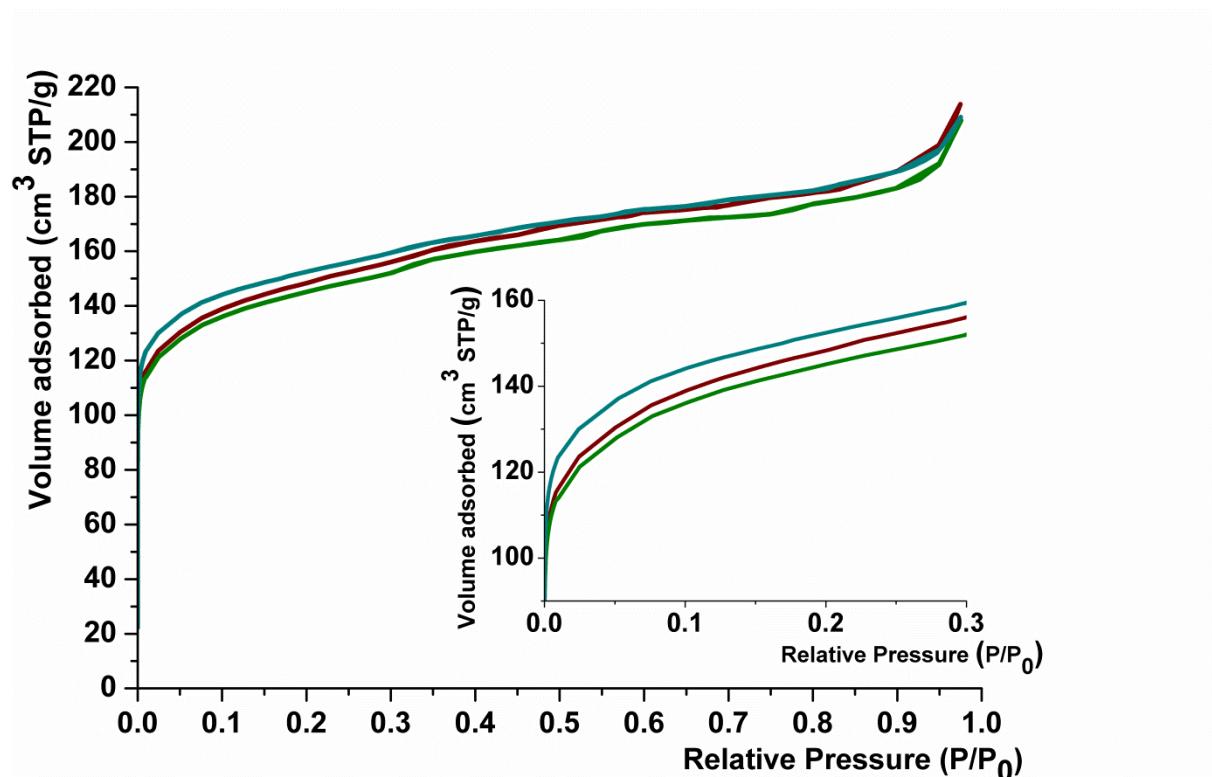
Figure S4 : Nitrogen adsorption and desorption isotherm of -COK-14(H1) (red), -COK-14(H2) (green) and COK-14 (C1) (blue). The inset shows a zoom in the 0 to 0.3 relative pressure region. -COK-14(H1) and -COK-14(H2) have a similar micropore volume (0.146 and 0.145 mL/g, respectively) and pore size (0.67 and 0.68 nm, respectively), substantially different from the fully connected sample COK-14(C1) having a pore volume of 0.160 mL/g and a pore size of 0.78 nm.

Figure S5
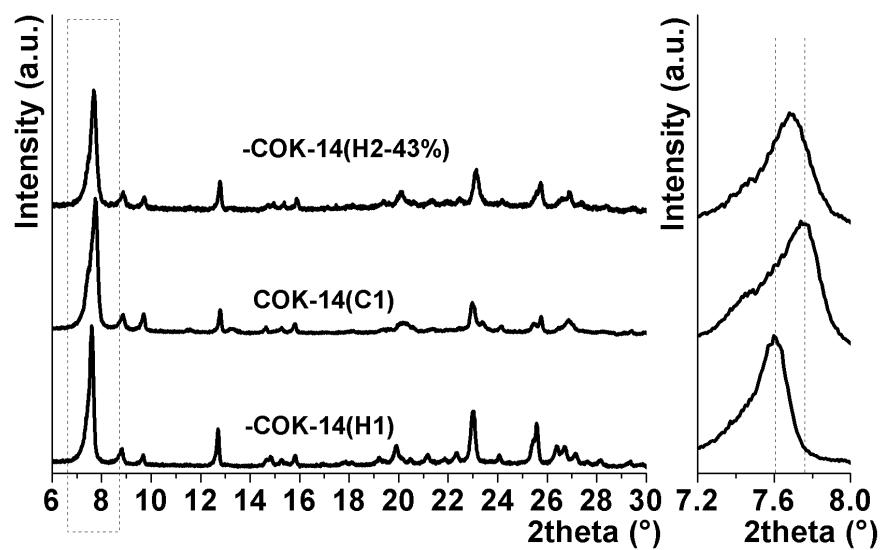
Figure S5 : X-ray diffraction patterns of parent -COK-14(H1), COK-14(C1) and -COK-14(H2-43%) zeolite. Magnification of the 7.2 - 8° 2theta range highlights the shifting of the 2 0 0 reflection between 7.6 and 7.77° 2theta during reversible framework transformation, indicated by the dashed lines. -COK-14(H2-43%) is only partial reopened as evidenced by the 2 0 0 reflection at 7.69° 2theta.

Table S1 : Listing of h k l reflections, 2theta positions, d spacings and relative intensities of -COK-14 and COK-14 zeolite in the 2 – 30° 2theta range. -COK-14 has a unit cell of to a = 24.6355(10) Å, b = 13.93666(23) Å, c = 12.2637(4) Å and an monoclinic angle β of 109.2189(33)° with a space group C 2/m and COK-14 a = 24.1319(15), Å, b = 13.7918(6) Å, c = 12.2977(4) Å and a monoclinic angle β of 109.600(4)° with a space group C 2/m

| -COK-14				COK-14			
h k l reflection	2theta (°)	d spacing (Å)	Intensity (%)	h k l reflection	2theta (°)	d spacing (Å)	Intensity (%)
1 1 0	7,392	11,96	3,43	1 1 0	7,495	11,79	18,28
2 0 0	7,598	11,63	100,00	0 0 1	7,629	11,59	11,41
0 0 1	7,632	11,58	11,29	2 0 0	7,775	11,37	100,00
2 0 -1	8,823	10,02	12,39	2 0 -1	8,882	9,95	10,89
1 1 -1	9,690	9,13	3,39	1 1 -1	9,724	9,09	10,22
1 1 1	11,499	7,69	2,03	1 1 1	11,599	7,63	2,59
2 0 1	12,431	7,12	0,53	2 0 1	12,603	7,02	0,05
0 2 0	12,699	6,97	20,89	0 2 0	12,833	6,90	7,25
3 1 0	13,061	6,78	0,07	3 1 -1	13,271	6,67	0,02
3 1 -1	13,099	6,76	0,32	3 1 0	13,327	6,64	4,07
4 0 -1	14,617	6,06	0,19	2 0 -2	14,646	6,05	1,94
2 0 -2	14,670	6,04	2,62	4 0 -1	14,877	5,95	0,03
2 2 0	14,815	5,98	3,73	0 2 1	14,946	5,93	0,11
0 2 1	14,832	5,97	5,03	2 2 0	15,022	5,90	0,65
4 0 0	15,230	5,82	3,43	0 0 2	15,291	5,79	2,23
0 0 2	15,297	5,79	2,81	4 0 0	15,586	5,68	0,01
2 2 -1	15,484	5,72	5,00	2 2 -1	15,628	5,67	0,19
1 1 -2	15,832	5,60	10,81	1 1 -2	15,823	5,60	3,20
3 1 1	16,949	5,23	5,26	3 1 -2	17,094	5,19	0,15
3 1 -2	17,037	5,20	0,09	3 1 1	17,226	5,15	0,00
4 0 -2	17,698	5,01	0,66	4 0 -2	17,818	4,98	0,01
2 2 1	17,806	4,98	3,50	2 2 1	18,024	4,92	0,10
1 1 2	18,111	4,90	2,10	1 1 2	18,194	4,87	0,36
5 1 -1	19,149	4,63	0,04	2 0 2	19,386	4,58	0,90
4 0 1	19,194	4,62	0,04	5 1 -1	19,511	4,55	0,07
2 0 2	19,234	4,61	4,80	2 2 -2	19,518	4,55	0,03
4 2 -1	19,408	4,57	2,26	4 0 1	19,563	4,54	0,35
2 2 -2	19,448	4,56	0,09	4 2 -1	19,694	4,51	0,23
1 3 0	19,478	4,56	0,25	1 3 0	19,694	4,51	1,13
4 2 0	19,878	4,46	18,67	0 2 2	20,011	4,44	0,52
0 2 2	19,930	4,45	0,15	4 2 0	20,240	4,39	11,82
5 1 0	20,113	4,41	6,04	5 1 0	20,560	4,32	0,99
1 3 -1	20,477	4,34	1,60	1 3 -1	20,662	4,30	0,62
5 1 -2	21,154	4,20	8,22	5 1 -2	21,383	4,15	1,53
1 3 1	21,407	4,15	0,02	1 3 1	21,622	4,11	0,32
6 0 -1	21,636	4,11	0,04	2 0 -3	21,671	4,10	0,08
2 0 -3	21,732	4,09	0,17	4 2 -2	22,018	4,04	1,57
4 2 -2	21,841	4,07	3,24	6 0 -1	22,093	4,02	0,01
3 3 0	22,299	3,99	9,47	3 3 -1	22,579	3,94	0,16
3 3 -1	22,322	3,98	0,28	3 3 0	22,613	3,93	1,93
3 1 2	22,884	3,88	3,65	1 1 -3	22,943	3,87	2,74
6 0 0	22,928	3,88	10,44	3 1 -3	22,977	3,87	4,11
1 1 -3	22,972	3,87	1,17	0 0 3	23,021	3,86	4,94
3 1 -3	22,993	3,87	2,89	4 0 -3	23,089	3,85	4,14

h	k	l				h	k	l			
6	0	-2	23,016	3,86	3,01	3	1	2	23,143	3,84	0,16
0	0	3	23,031	3,86	20,10	2	2	2	23,316	3,81	0,15
4	0	-3	23,072	3,85	16,08	6	0	-2	23,338	3,81	0,42
4	2	1	23,080	3,85	2,79	4	2	1	23,464	3,79	3,53
2	2	2	23,113	3,85	0,61	6	0	0	23,469	3,79	3,29
5	1	1	23,701	3,75	0,04	5	1	1	24,170	3,68	0,42
1	3	-2	24,054	3,70	4,08	1	3	-2	24,193	3,68	2,67
3	3	1	24,816	3,59	0,00	3	3	-2	25,056	3,55	0,26
3	3	-2	24,877	3,58	0,00	3	3	1	25,148	3,54	0,01
4	0	2	25,008	3,56	0,00	2	2	-3	25,263	3,52	0,09
6	2	-1	25,163	3,54	0,07	4	0	2	25,359	3,51	0,16
2	2	-3	25,246	3,53	0,00	1	1	3	25,477	3,49	1,91
1	1	3	25,406	3,50	10,17	5	1	-3	25,570	3,48	1,73
5	1	-3	25,463	3,50	11,31	6	2	-1	25,629	3,47	1,08
0	4	0	25,554	3,48	25,88	0	4	0	25,827	3,45	4,22
1	3	2	25,637	3,47	0,95	1	3	2	25,832	3,45	0,69
7	1	-1	26,127	3,41	0,35	0	2	3	26,440	3,37	0,69
6	2	0	26,292	3,39	6,03	4	2	-3	26,499	3,36	0,33
6	2	-2	26,369	3,38	12,24	7	1	-1	26,683	3,34	0,36
0	2	3	26,382	3,38	0,98	6	2	-2	26,719	3,33	2,38
5	3	-1	26,392	3,38	0,66	2	0	3	26,743	3,33	0,76
4	2	-3	26,418	3,37	3,28	5	3	-1	26,791	3,33	0,88
6	0	1	26,525	3,36	3,19	6	2	0	26,834	3,32	1,40
2	0	3	26,604	3,35	2,89	6	0	-3	26,860	3,32	0,56
6	0	-3	26,677	3,34	1,85	0	4	1	26,966	3,30	1,33
2	4	0	26,695	3,34	10,15	2	4	0	27,010	3,30	6,81
0	4	1	26,705	3,34	1,07	6	0	1	27,090	3,29	0,28
7	1	-2	26,928	3,31	3,72	7	1	-2	27,360	3,26	0,52
2	4	-1	27,082	3,29	1,02	2	4	-1	27,360	3,26	0,09
5	3	0	27,111	3,29	12,03	5	3	0	27,578	3,23	1,75
7	1	0	27,579	3,23	2,65	5	3	-2	28,207	3,16	0,49
5	3	-2	27,904	3,20	0,15	7	1	0	28,214	3,16	1,90
4	2	2	28,138	3,17	6,00	4	2	2	28,515	3,13	1,32
2	4	1	28,507	3,13	0,00	2	4	1	28,831	3,09	0,18
5	1	2	29,001	3,08	0,00	2	0	-4	29,135	3,06	0,92
8	0	-1	29,079	3,07	1,05	1	3	-3	29,426	3,03	1,14
2	0	-4	29,216	3,05	1,09	3	3	-3	29,453	3,03	0,44
3	3	2	29,259	3,05	0,67	5	1	2	29,459	3,03	0,25
1	3	-3	29,329	3,04	2,76	4	0	-4	29,529	3,02	0,01
3	3	-3	29,346	3,04	1,29	3	3	2	29,585	3,02	0,11
8	0	-2	29,471	3,03	0,15	8	0	-1	29,734	3,00	0,07
6	2	1	29,505	3,03	0,48	2	2	3	29,762	3,00	0,35
4	4	-1	29,558	3,02	0,18	3	1	-4	29,790	3,00	0,14
2	2	3	29,577	3,02	0,00	2	4	-2	29,811	3,00	0,00
4	0	-4	29,579	3,02	0,01	6	2	-3	29,869	2,99	0,01
2	4	-2	29,585	3,02	0,86	4	4	-1	29,930	2,98	0,00
6	2	-3	29,643	3,01	0,00	3	1	3	29,973	2,98	1,28
3	1	3	29,732	3,00	1,63	8	0	-2	30,004	2,98	0,01
7	1	-3	29,814	2,99	0,93						
3	1	-4	29,852	2,99	0,05						
4	4	0	29,876	2,99	1,88						
0	4	2	29,912	2,99	0,14						
5	3	1	29,913	2,99	0,23						
1	1	-4	30,496	2,93	0,00						

Table S2

Table S2 : ^{29}Si isotropic chemical shift (ppm) and relative intensity (%) of the Q^n resonances of the -COK-14(H1) and COK-14(C1) (deconvolution of ^{29}Si MAS NMR spectra of Figure 4, main manuscript)

Sample Name	Q^3 (ppm)	Q^4 (ppm)	Q^4 (ppm)
-COK-14(H1)	-101 (13%)	-111 (87%)	
COK-14(C1)	-100 (4%)	-109 (81%)	-114 (15%)

References

1. D. Massiot, F. Fayon, M. Capron, I. King, S. Le Calvé, B. Alonso, J.-O. Durand, B. Bujoli, Z. Gan, and G. Hoatson, *Magn. Reson. Chem.*, 2002, **40**, 70.
2. G. Halsey, *J. Chem. Phys.*, 1948, **16**, 931.
3. A. Saito and H. C. Foley, *AIChe*, 1991, **37**, 429.
4. G. Kresse and J. Hafner, *Phys. Rev. B*, 1994, **49**, 1425.
5. G. Kresse and J. Furthmüller, *Comput. Mater. Sci*, 1996, **6**, 15.
6. P. E. Blöchl, *Phys. Rev. B*, 1994, **50**, 17953.
7. G. Kresse and D. Joubert, *Phys. Rev. B*, 1999, **59**, 11.
8. J. Perdew, K. Burke, and M. Ernzerhof, *Phys. Rev. Lett.*, 1996, **77**, 3865.
9. G. Piccini and J. Sauer, *J. Chem. Theory Comput.*, 2013, **9**, 5038.
10. A. Ghysels, D. Van Neck, V. Van Speybroeck, T. Verstraelen, and M. Waroquier, *J. Chem. Phys.*, 2007, **126**, 224102.
11. J. D. Gale, *J. Chem. Soc., Faraday Trans.*, 1997, **93**, 629.
12. M. J. Sanders, M. Leslie, and C. R. A. Catlowb, *J. Chem. Soc., Chem. Commun.*, 1984, 1271.
13. H. T. Stokes and D. M. Hatch, *J. Appl. Cryst.*, 2005, **38**, 237.